# Rapid Musculoskeletal MRI in 2021: Value and Optimized Use of Widely Accessible Techniques

Filippo Del Grande, MD[1], Roman Guggenberger, MD[2], Jan Fritz, MD[3]

Musculoskeletal Imaging · Review

**Keywords**

acceleration, accessible, fast MRI, gradients, MRI

Submitted: Feb 3, 2020
Revision requested: Feb 12, 2020
Revision received: May 18, 2020
Accepted: May 31, 2020

F. Del Grande and R. Guggenberger received institutional research support from Siemens Healthcare. J. Fritz received institutional research support from Siemens Healthcare USA, DePuy, Zimmer, Microsoft, BTG International, SyntheticMR, and Quality Electrodynamics; served as a scientific advisor to Siemens Healthcare USA, GE Healthcare Technologies, BTG International, Quality Electrodynamics, ImageBiopsy Labs, SyntheticMR, and Mirata Pharma; received a speaker's honorarium from Siemens Healthcare USA and GE Healthcare; and has shared patents with Siemens Healthcare and Johns Hopkins University.

**OBJECTIVE.** The purpose of this article is to provide a practice-focused review of accelerating musculoskeletal MRI with the use of widely accessible techniques and to assess the effects of such acceleration on the value of musculoskeletal MRI.

**CONCLUSION.** Echo-train compaction with fast radiofrequency pulses, high gradient performance modes, and high receiver bandwidth, as well as basic phase undersampling techniques, affords at least twofold acceleration of musculoskeletal MRI examinations while retaining image quality, comprehensiveness, and diagnostic performance. Optimized efficiency is a cornerstone for adding value to musculoskeletal MRI.

MRI provides tremendous value to the practice of sports medicine and orthopedic surgery because of its high accuracy in the detection, diagnosis, characterization, and surveillance of a broad spectrum of conditions, injuries, and diseases of the bone, tendons, ligaments, muscles, connective tissues, and nerves [1–7]. Because of its unparalleled soft-tissue contrast, MRI excels as an imaging modality, particularly when injuries and other abnormalities are suspected but findings from the patient's history, clinical examination, and other imaging studies are inconclusive [8–11].

Although image quality and the radiologist having adequate expertise are factors critical in diagnostic performance, valuation of musculoskeletal MRI is subject to additional factors [12]. Optimized efficiency is an essential cornerstone for several value-defining factors that permit retaining and further increasing the value of musculoskeletal MRI by expanding its availability and accessibility, improving tolerability, reducing motion artifacts, decreasing needs for sedation and anesthesia, and augmenting throughput [13–15].

Since the invention of MRI, increasing the speed of MRI has been at the center of research and development efforts [13]. Today, a wide variety of techniques are available from various vendors, and these techniques can be categorized as hardware- and software-based solutions. Advances in scanner and coil technologies, including high-performance gradients, refined radiofrequency pulse techniques, and multichannel technology, redefine the baseline capabilities of rapid MRI acquisitions and contribute to fast spin-echo (FSE) and turbo spin-echo (TSE) pulse sequences to reach the highest levels of efficiency and image quality [14].

In this article, the first in a series of two, we focus on how to optimize the use of modern scanner technology and widely accessible acceleration techniques to shorten musculoskeletal MRI examinations while retaining their comprehensiveness and image quality. The widely accessible techniques that we describe are available on most MRI scanners and platforms and usually do not require advanced licensing.

The second article in this series [16] focuses on the clinical use and applications of advanced and newer techniques in further accelerating musculoskeletal MRI examinations, including parallel imaging, simultaneous multislice acceleration, compressed sensing–based methods, synthetic MRI techniques, and artificial intelligence–based image reformation techniques [15]. However, some of the newer techniques require advanced licensing and dedicated receiver coils, which may not be available on all platforms and in all regions [17].

The purpose of this article is to provide a practice-focused review of how to accelerate musculoskeletal MRI examinations through the combined utilization of modern scanner

doi.org/10.2214/AJR.20.22901
*AJR* 2021; 216:1–14
ISSN-L 0361–803X/21/2163–1


[1]Radiology Clinic, Imaging Institute of Southern Switzerland, Lugano, Ticino, Switzerland.

[2]Department of Diagnostic and Interventional Radiology, University Hospital Zurich, Zurich, Switzerland.

[3]Department of Radiology, Division of Musculoskeletal Radiology, NYU Grossman School of Medicine, 660 1st Ave, 3rd Fl, Rm 313, New York, NY 10016. Address correspondence to J. Fritz (jan.fritz@nyulangone.org).

technology and widely accessible techniques and to review the effects of such acceleration on the value of musculoskeletal MRI.

## Value Considerations

Increasing scrutiny of health care utilization, efforts to decrease health care expenditures, and projected obligations to deliver the best possible care at a lower cost have contributed to challenges to and reevaluation of the value of MRI. The complex and multidimensional valuation of MRI extends from a global effort to increase accessibility, value for money, and the impact on patient management [12] to requirements to prove that MRI favorably changes treatment decisions, improves patient outcomes, and is cost-effective [18].

The number of musculoskeletal MRI examinations has continually increased over the past decades, as exemplified by a 354% increase in musculoskeletal MRI examinations reimbursed by Medicare from 1996 to 2005, with the cost of such examinations projected to be $2 billion in 2020 [19]. Meanwhile, reimbursements for musculoskeletal MRI examinations have been decreasing over the past decade, as exemplified by an inflation-adjusted 60% reduction in professional and technical reimbursements for MRI examinations of the upper extremity between 2007 and 2015 [20].

In addition to diagnostic performance, efficiency is critical in retaining and adding to the value of musculoskeletal MRI [13]. For efficiency purposes, the time required to perform MRI examinations can be categorized as gradient time (value-added time) and nongradient time (business and non–value-added time). Nongradient time, with an average duration of 20 minutes [21], can be reduced to 5 minutes or less through innovative architectural design of imaging sites and by equipping MRI systems with two dockable tables and multiple receiver coils [22]. With the use of such a setup, patients can undergo preparation for their examination and be positioned on the table outside the MRI room while another examination is in progress.

Gradient times depend on technologic, operational, and health care environment–related factors but may average 20–30 minutes for musculoskeletal MRI examinations performed in a traditional setting [21, 23]. Gradient time may occupy more than 50% of the total duration of musculoskeletal MRI examinations [21], providing opportunities to add value through improving efficiency.

Although increasing efficiency remains a cornerstone for adding value to musculoskeletal MRI, improvements in efficiency ideally should retain image quality as well as the comprehensiveness of MRI examinations. The practical effects of shorter musculoskeletal MRI examinations are increasing availability and tolerability, decreasing motion artifacts, reduced needs for sedation and anesthesia, higher throughput, shorter patient contact times during pandemics (such as the coronavirus disease [COVID-19] pandemic), and potentially the ability to decrease the technical cost of examinations [24, 25].

Accelerating MRI protocols requires careful negotiation between spatial, temporal, and contrast resolutions, which define image quality and, ultimately, diagnostic performance and value. At the center of this negotiation is the available signal-to-noise ratio (SNR), which serves as a surrogate marker for the overall signal observed on MR images. Shifting this dynamic association toward faster imaging while preserving image contrast and spatial resolution as much as possible is the challenge faced when designing rapid MRI protocols.

Simple strategies to reduce gradient time consist of decreasing the number of pulse sequences, plane orientations, and contrast weightings; reducing TRs; and reducing spatial resolution by enlarging voxel size, increasing slice thickness, and widening interslice gaps to the lowest standard to match existing guidelines [26]. This approach, however, may create a decline in the value of MRI caused by the production of a higher number of lower-quality images that potentially have a lower accuracy for detecting abnormalities, a higher risk of missed findings, and ultimately a diminished quality of patient care [27].

Different strategies to reduce the gradient time of musculoskeletal MRI capitalize on an often present but difficult-to-recognize excess of SNR that is created by several factors, including the use of FSE and TSE pulse sequences, wrap-avoiding phase and slice oversampling, 3-T field strength, surface coils, and contrast- and signal-preserving long TRs and intermediate TEs. Excess SNR offers numerous opportunities to accelerate image acquisition with preservation of or only modest reductions in TR and voxel size, constant anatomic coverage, and retention of contrast resolutions.

Improving efficiency has several positive implications for the value of musculoskeletal MRI; however, for interpreting radiologists, the effects of rapid MRI examinations require careful consideration and management. Accelerated musculoskeletal MRI can lead to a substantial increase in the daily number of examinations performed. In the absence of practice expansion, adverse effects can include increased levels of stress, unwellness, and burnout among musculoskeletal radiologists. A study that surveyed members of the Society of Skeletal Radiology found a cautionary 80% prevalence of at least one of three burnout symptoms (emotional exhaustion, depersonalization, or a perceived lack of personal accomplishment) among musculoskeletal radiologists [28].

## Associations Between Acquisition Time and Pulse Sequence Parameters

When widely accessible techniques are applied to accelerate musculoskeletal MRI examinations, simplified proportional relationships between pulse sequence parameters and acquisition times can be helpful in accurately predicting effects on the acquisition time, as illustrated by the following equation:

$$\text{Acquisition time} \approx \frac{NSA \times TR \times N_y \times N_{SL} \times RES_{PE} \times RES_{SL}}{ETL \times PFP}, \quad (1)$$

where *NSA* is the number of signals acquired or the number of times an image is repeated and averaged, $N_y$ is the number of in-plane phase-encoding steps, $N_{SL}$ is the number of phase-encoding steps in slice direction (and applies to 3D volume acquisitions only), $RES_{PE}$ is the phase resolution relative to the frequency encoding direction, $RES_{SL}$ is the phase resolution in slice direction (and applies to 3D volume acquisitions only), *ETL* is the echo-train length or turbo factor (indicating the number of echoes sampled within one TR), and *PFP* is the partial Fourier phase or zero filling factor.

## Field Strength and Number of Signals Acquired

With allowance for small differences [29], musculoskeletal MRI examinations can be successfully performed using different field strengths [30]. However, field strength is a critical factor in rapid

musculoskeletal MRI. Compared with a field strength of 1.5 T, a field strength of 3 T permits MRI to be performed approximately four times faster but achieves a similar SNR. This relationship is based on the approximately twofold higher SNR yield achieved with 3 T [31], which, when compared with 1.5 T, requires four times the number of signals acquired.

## TR and Contrast Considerations

Proton density–weighted, or intermediate-weighted, FSE and TSE pulse sequences are advantageous for diagnosing a broad variety of musculoskeletal conditions because of three core properties: their ability to achieve high signal gains; display fluid as hyperintense (i.e., fluid sensitivity) to detect and characterize abnormalities associated with high-signal-intensity edema, inflammation, and collections; and attain high contrast differentiation of musculoskeletal tissues that naturally have lower concentrations of protons, long T1 constants, and short T2 constants, including ligaments, tendons, and articular cartilage and fibrocartilage [32].

For 2D FSE and TSE pulse sequences, the three aforementioned core properties depend on the choice of appropriate TE and a sufficiently long TR. The use of intermediate TEs of 20–45 ms allow sampling of signal-rich echoes for contrast weighting, which results in a high signal gain and high contrast differentiation of musculoskeletal tissues. Sufficiently long TRs of 3500–5000 ms maximize desirable T2 contrast effects and minimize undesirable T1 contrast effects [33], which form the basis for the fluid sensitivity. Furthermore, long TRs recover more longitudinal magnetization and result in a higher SNR [34].

Because TR directly relates to the acquisition time (see equation 1), minimizing TR to shorten sequence acquisition is tempting. Although the effects are often small (between 3500 and 4500 ms for proton density– and T2-weighted FSE and TSE pulse sequences), reductions in TR to less than 3000 ms often result in visibly reduced fluid signal intensity and low contrast differentiation of musculoskeletal tissues. A more favorable strategy for musculoskeletal MRI is to retain long TRs and use the high signal gain to apply acceleration techniques while retaining favorable proton density– and T2-weighted contrasts, including fluid sensitivity.

When using 3D FSE and TSE pulse sequences, the combination of long echo trains and complex flip angle modulation schemes permits much shorter TRs that can still achieve proton density–weighted image contrast [35–37].

## Fast Spin-Echo and Turbo Spin-Echo Pulse Sequences

Conventional spin-echo pulse sequences produce excellent spatial and contrast resolution of musculoskeletal structures; however, long TRs and the number of phase-encoding steps result in very long acquisition times (see equation 1). For this reason, the emergence of the RARE technique in 1986 represented one of the most influential discoveries for accelerating spin-echo and other pulse sequences [38]. Today, most vendors offer this technique as FSE or TSE pulse sequences.

Although spin-echo pulse sequences acquire only one echo during every TR, FSE and TSE pulse sequences sample multiple echoes and thus allow much faster scanning. The number of echoes for each TR (i.e., the echo-train length [ETL] or turbo factor) is inversely proportional to the acquisition time (see equation 1), which means that an ETL of 5 reduces the time to acquire a conventional spin-echo image by approximately 80%. Consequently, increasing the ETL of FSE and TSE pulse sequences from 5 to 10 constitutes twofold acceleration.

The advantages of using FSE and TSE pulse sequences for musculoskeletal MRI are manifold and include the ability to generate proton density–, T1-, and T2-weighted contrasts; add spectral and STIR fat suppression techniques [39]; attain high signal and achievable high spatial resolution; be combined with advanced metal artifact suppression techniques [40, 41]; and be applied to a broad variety of acceleration methods.

Any pulse sequence and acceleration technique should be executed within recommended specific absorption rate (SAR) limits [42]. Because multiple refocusing pulses are used to generate the echoes of FSE and TSE pulse sequences, the imparted radiofrequency energy initially increases with longer echo trains, and SAR limits may be approached more quickly. Different strategies to reduce the SAR exist, and these include lowering the degree of refocusing flip angles, using lower-energy flip angle designs, increasing the TR, and reducing the number of slices [43]. For achieving rapid MRI examinations, reducing refocusing flip angles is the best choice because a nonlinear relationship with the SAR exists. In practical terms, the use of refocusing flip angles of 125–150°, rather than 180°, often has little influence on perceptible image quality.

The number of echoes obtained during one TR of FSE and TSE pulse sequences (i.e., the ETL) is one of the most potent means of reducing the scanning time because the number of echoes within an echo train is directly and inversely proportional to the acquisition time (see equation 1). However, certain considerations apply when choosing the ETL. Although the effective TE determines which echoes define the contrast of the MR image, peripheral echoes within the echo train also contribute to contrast, and longer echo trains thus inherently increase the T2-weighting of the MR image. Although this often is an acceptable or even desired effect of musculoskeletal MRI when using FSE and TSE pulse sequences with intended fluid sensitivity, achieving T1 contrast with FSE and TSE pulse sequences requires limiting ETLs to 3 or 4.

## Gradient Performance, Radiofrequency Pulse Speed, and Echo-Train Length

Although typically not included in time association equations for MRI (see equation 1), gradient performance, radiofrequency pulse speed, and receiver bandwidth are essential factors for rapid musculoskeletal MRI. All three parameters can be chosen by the operator and can determine echo spacing, which is the most critical component that defines how fast an FSE or TSE pulse sequence can produce and record MR signals and how long echo trains can be used to produce high-quality images.

The magnetic gradient fields of an MRI scanner prepare and modify MR signals for recording and image creation. The quality of a gradient system is indicated by the gradient speed (i.e., slew rate [T/m/s]) and gradient strength (mT/m), which indicate how quickly and how powerfully gradient effects can be achieved [44]. Modern clinical MRI scanners with slew rates of 150–200 T/m/s and gradient strengths of 35–80 mT/m permit much faster execution of FSE and TSE pulse sequences much faster than was possible in previous generations (Fig. 1), which is of critical importance for rapid musculoskeletal MRI. Gradients have no direct effects on the SAR. Although patients may experience nerve-stimulating effects when

higher gradient performance modes are used [45], these effects are usually well tolerated during musculoskeletal MRI.

Within FSE and TSE pulse sequences, many radiofrequency pulses are used to generate recordable MR signals. Modern scanners allow the user to choose between different radiofrequency pulse modes, which define how fast the radiofrequency pulses will be executed within the FSE and TSE pulse sequences. Radiofrequency pulses with shorter durations require less time, shorten echo spacing, and result in faster sampling (Fig. 1). When compared with slower modes, faster radiofrequency pulses may impart more energy and may contribute to a higher SAR.

The receiver bandwidth defines how fast an MRI scanner can record MR signals. As such, high bandwidths also permit faster sampling of MR signals (Fig. 1). Additional positive effects are reduced chemical-shift artifacts and improved sharpness of MR images. A high receiver bandwidth results in an overall lower strength of the MR signal and a reduced SNR. However, the associated shortening of echo spacing leads to earlier sampling of stronger MR signals, which limits SNR loss.

The combined use of high-performance gradients, fast radiofrequency pulses, and high receiver bandwidth drastically shortens echo spacing, which is one of the most powerful and widely accessible techniques for performing rapid, high-quality musculoskeletal MRI. The shorter acquisition time of FSE and TSE pulse sequences results from the ability to shorten long TRs (see equation 1) (Figs. 1 and 2 and Table 1), sample more echoes within the same amount of time (see equation 1) (Figs. 3 and 4 and Table 2), and combinations thereof.

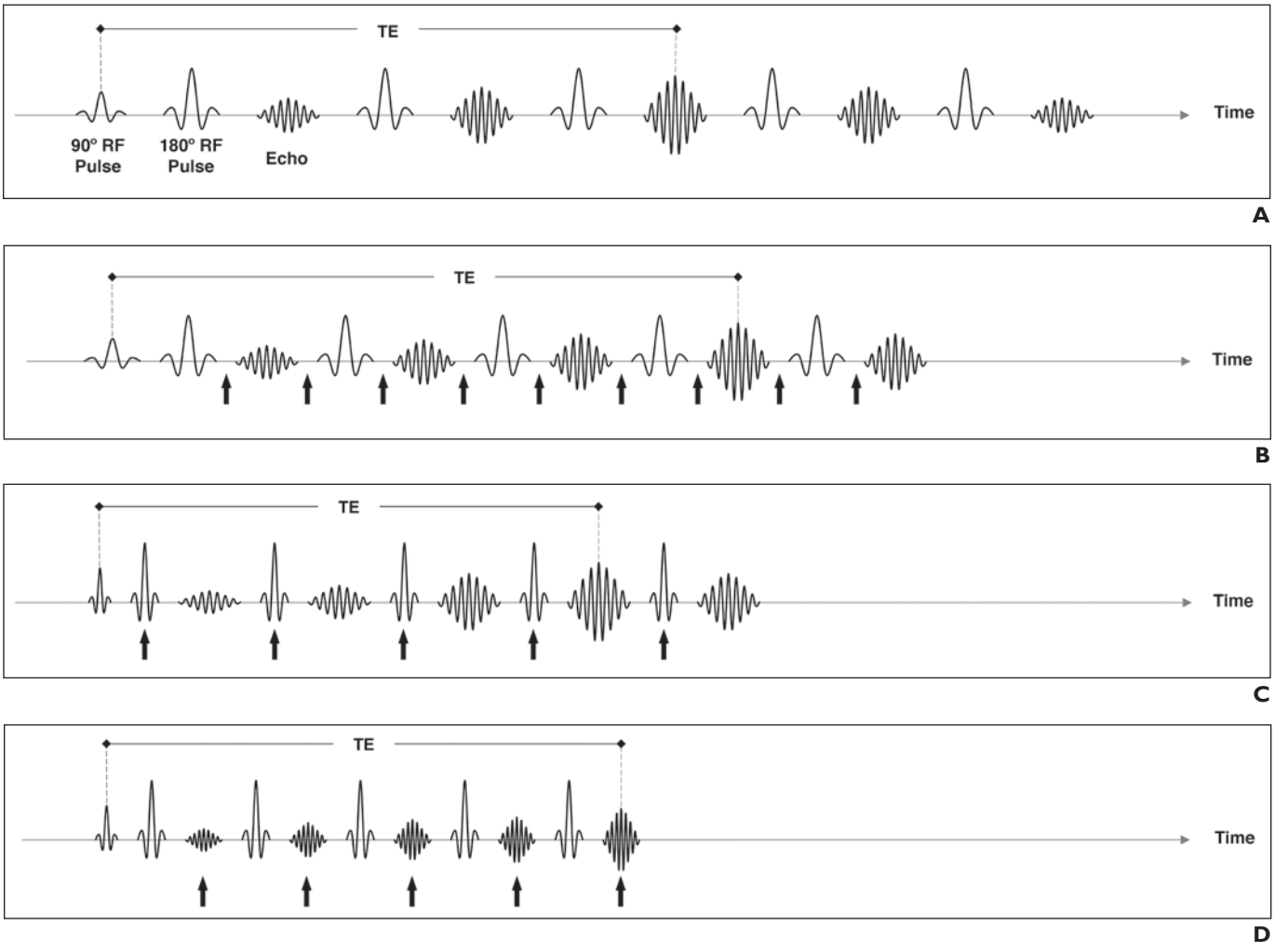


**Fig. 1**—Effects of strong gradients, fast radiofrequency (RF) pulses, and high-readout bandwidth on fast spin-echo and turbo spin-echo pulse sequences.
**A,** Schematic shows baseline fast spin-echo and turbo spin-echo pulse sequence consisting of series of RF pulses and echoes and effective TE.
**B,** Schematic shows that when faster and stronger gradients are applied to same pulse sequence, time gaps (*arrows*) between RF pulse and echoes shorten, which accelerates completion of echo train (i.e., shorter time to complete echo train).
**C,** Schematic shows that when additional fast RF pulses are applied, RF pulse lengths shorten (*arrows*), which leads to further shortening of time to complete echo train.
**D,** Schematic shows that when high readout bandwidth is added, lengths of individual echoes shorten (*arrows*), which leads to further shortening of time to complete echo train. Note that use of higher-readout bandwidth reduces signal strength of each echo (i.e., reduces amplitude height), which is often outweighed by benefits of faster readouts of high-signal echoes, reduced chemical-shift effects, and decreased blurring. Each parameter (as shown in **A–C**) contributes to shortening of time between center of adjacent echoes (echo spacing), which permits shorter TRs. Side effects of shortening of echo-train length are small shifts in mathematically possible effective TE that can be selected by operator as fixed increments in sequence cards. Shifts usually occur within few milliseconds without having major influences on image contrast.

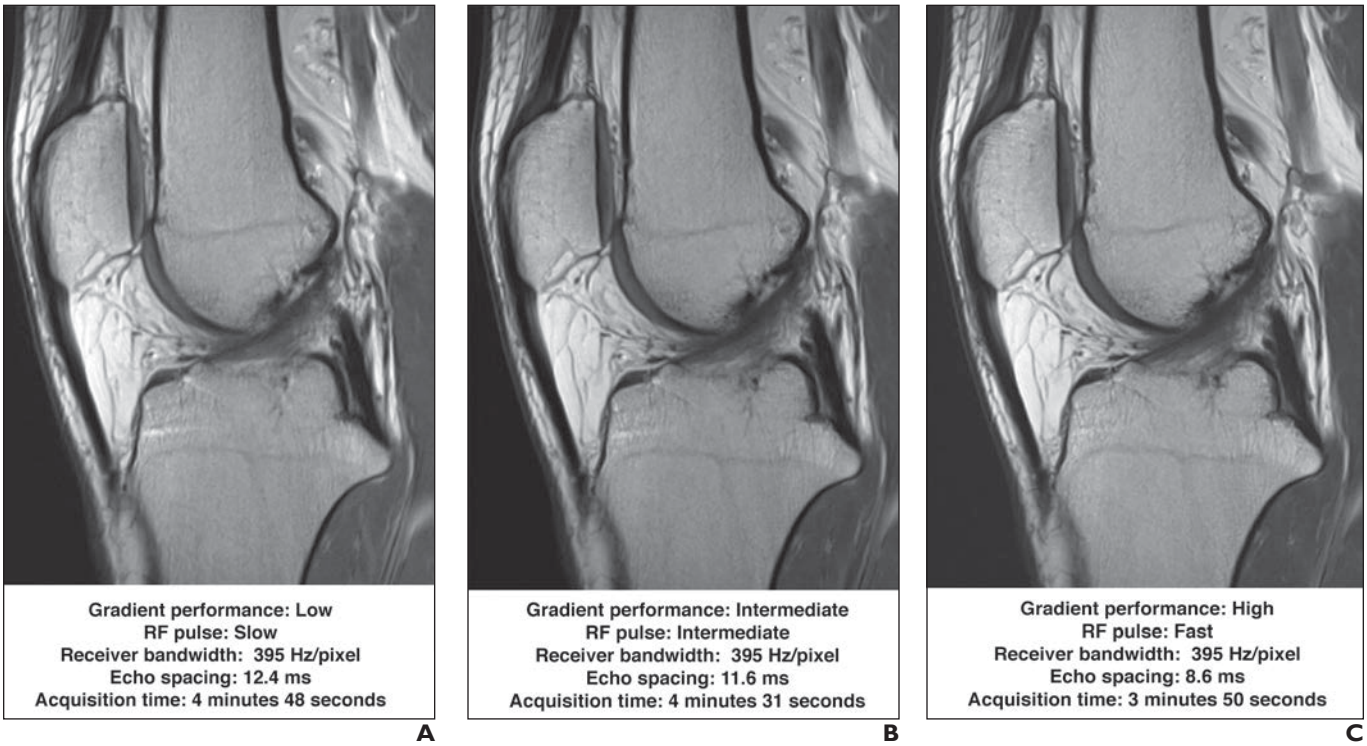


**Fig. 2**—32-year-old healthy man. Effects of gradient performance and radiofrequency (RF) pulse length on echo spacing and acquisition time using sagittal intermediate-weighted turbo spin-echo MR images of knee. Decreases in echo spacing caused by higher gradient performance and shorter RF pulses decreases blurring, shortens acquisition time by approximately 1 minute through reducing minimum TR lengths, and improves image quality.
**A,** MR image obtained with lowest gradient performance and widest echo spacing.
**B,** MR image obtained with intermediate gradient performance and closer echo spacing than in **A**.
**C,** MR image obtained with highest gradient performance and closest echo spacing.

**TABLE 1: Effects of Gradient Performance, Radiofrequency Pulse Length, and Receiver Bandwidth When Using Sagittal Proton Density–Weighted TSE Pulse MRI Sequences of the Knee**

| Parameter | Sequence 1 | Sequence 2 | Sequence 3 |
|---|---|---|---|
| Orientation | Sagittal | Sagittal | Sagittal |
| Gradient performance | Low | Intermediate | High |
| Radiofrequency speed | Slow | Intermediate | Fast |
| Minimum TR (ms) | 5030 | 4730 | 4010 |
| TE (ms) | 25 | 23 | 26 |
| Echo-train length | 12 | 12 | 12 |
| Bandwidth (Hz/pixel) | 395 | 395 | 395 |
| FOV (mm) | 150 × 150 | 150 × 150 | 150 × 150 |
| Matrix size | 386 × 386 | 386 × 386 | 386 × 386 |
| Slice thickness (mm) | 2.5 | 2.5 | 2.5 |
| Voxel size (mm) | 0.4 × 0.4 × 2.5 | 0.4 × 0.4 × 2.5 | 0.4 × 0.4 × 2.5 |
| No. of slices | 30 | 30 | 30 |
| No. of concatenations | 1 | 1 | 1 |
| Phase direction | Head to foot | Head to foot | Head to foot |
| Phase oversampling (%) | 75 | 75 | 75 |
| Flip angle (°) | 150 | 150 | 150 |
| Echo spacing (ms) | 12.4 | 11.6 | 8.6 |
| Acquisition time (min:s) | 4:48 | 4:31 | 3:50 |

Note—TSE = turbo spin-echo.

The combination of shortening the echo spacing and adding echoes to the echo train in a time-neutral fashion prevents the undesirable blurring effects of prolonged echo trains (Fig. 3). The net gains are shorter acquisition times and the preservation of image quality (Fig. 4). Longer TEs of 55–80 ms and higher matrix resolutions tolerate longer echo trains.

Three-dimensional pulse sequences require much longer echo trains to compensate for the longer acquisition times, which relate to the multiplied, high number of encoding steps in the phase, and partition directions [34]. Although excessively long echo trains degrade image quality through the introduction of edge blurring (Fig. 5), increasing T2 weighting and degrading the quality of multiplanar reformation images, high-spatial-resolution 3D FSE- and TSE-based pulse sequences tolerate substantially longer echo trains than do 2D sequences.

## Matrix Resolution Phase Undersampling

Forming an MR image requires the phase encoding of echoes. Unlike frequency encoding, phase encoding is time-consuming and is directly proportional to the acquisition time (see equation 1).

For 2D FSE and TSE echo sequences, there is one time-consuming, in-plane, phase-encoding direction, whereas the other in-plane and slice directions are frequency encoded (see equation 1). In contrast, 3D FSE and TSE sequences also have the slice or partition direction phase encoded, which results in a total of two time-consuming, phase-encoding directions (see equation 1). The total number of echoes with different phase-encoding steps subsequently determines the spatial resolution in a phase-encoding direction according to the maximally possible 2D and 3D matrix sizes. Because the number of phase-encoding steps is directly proportional to the acquisition times, reducing the number of phase-encoding steps is one of the most effective means of reducing the scanning time (see equation 1).

The shape of the picture elements (i.e., pixels) of MR images is usually quadratic; however, this is neither a technical requirement nor a convention of MRI. Rectangular pixels result from scanning with asymmetric matrices, which can be achieved by reducing the matrix size in the phase-encoding direction while keeping the FOV constant. For 3D TSE and FSE sequences, the reduction in one or both phase-encoding directions will change cubic (isotropic) voxels to rodlike (anisotropic) voxels. This strategy can be considered undersampling in a phase-encoding direction or oversampling in a frequency-encoding direction. The magnitude of phase matrix reductions is directly proportional to the acquisition time (see equation 1), whereas higher-frequency matrices have few effects on the acquisition time.

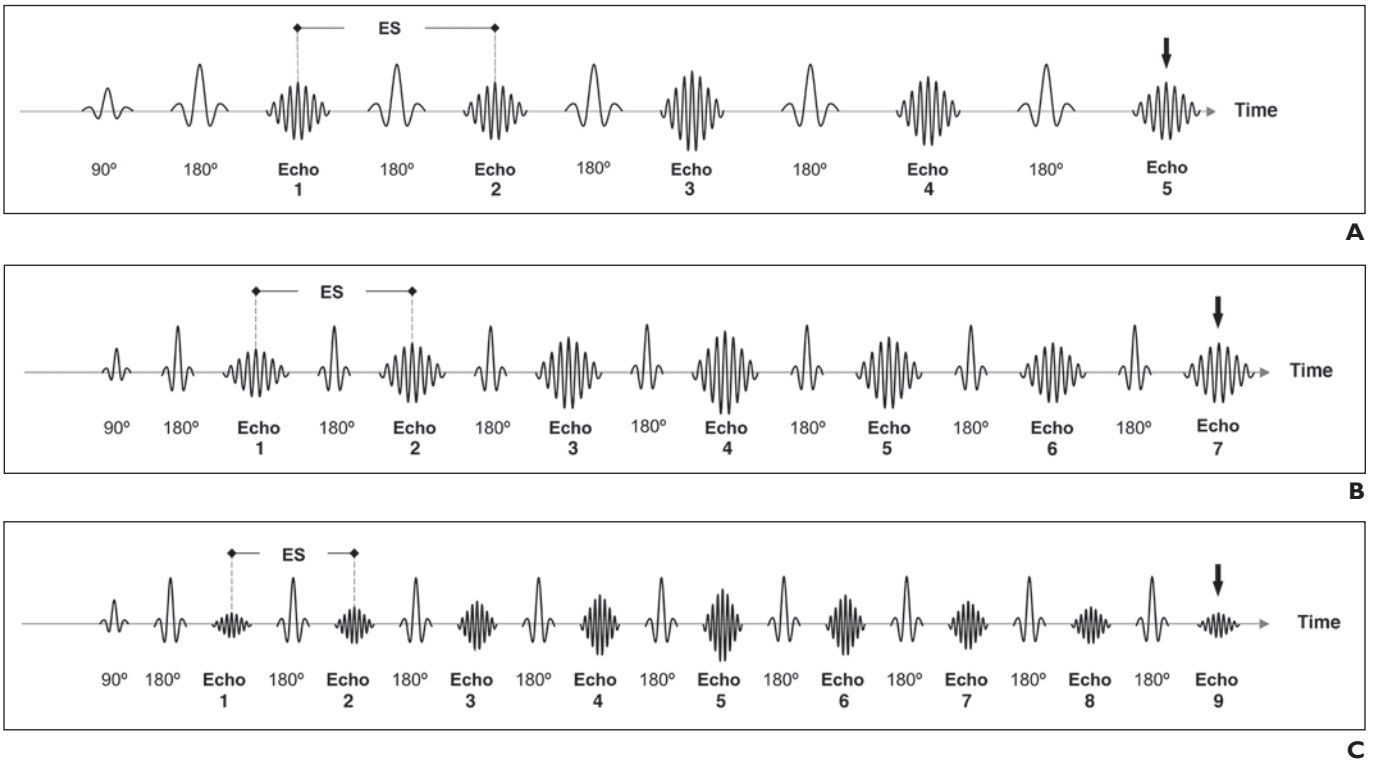


**Fig. 3**—Strategy for TR-neutral shortening of overall acquisition time. ES = echo spacing.
**A,** Schematic shows fast spin-echo and turbo spin-echo pulse sequences consisting of series of radiofrequency pulses (90° and 180°) and five echoes, ES at baseline, and length of time of echo train at baseline (*arrow*).
**B,** Schematic shows shortening of ES through use of stronger gradients and faster radiofrequency pulses, which permits sampling of two more echoes (echoes 6 and 7) within same length of time of echo train (*arrow*).
**C,** Schematic shows further shortening of ES through use of high receiver bandwidth permits sampling of two more echoes (echoes 8 and 9) within same length of time of echo train (*arrow*). Because almost twice number of echoes can now be acquired within same length of time of echo train, overall lower total number of echo trains is needed for sampling total number of images, which reduced overall acquisition time by 80%. This strategy is TR neutral because length of time that is required to complete each echo train is unchanged, which is useful to retain TRs for proton density and T2 contrast weighting and to preserve fluid sensitivity.

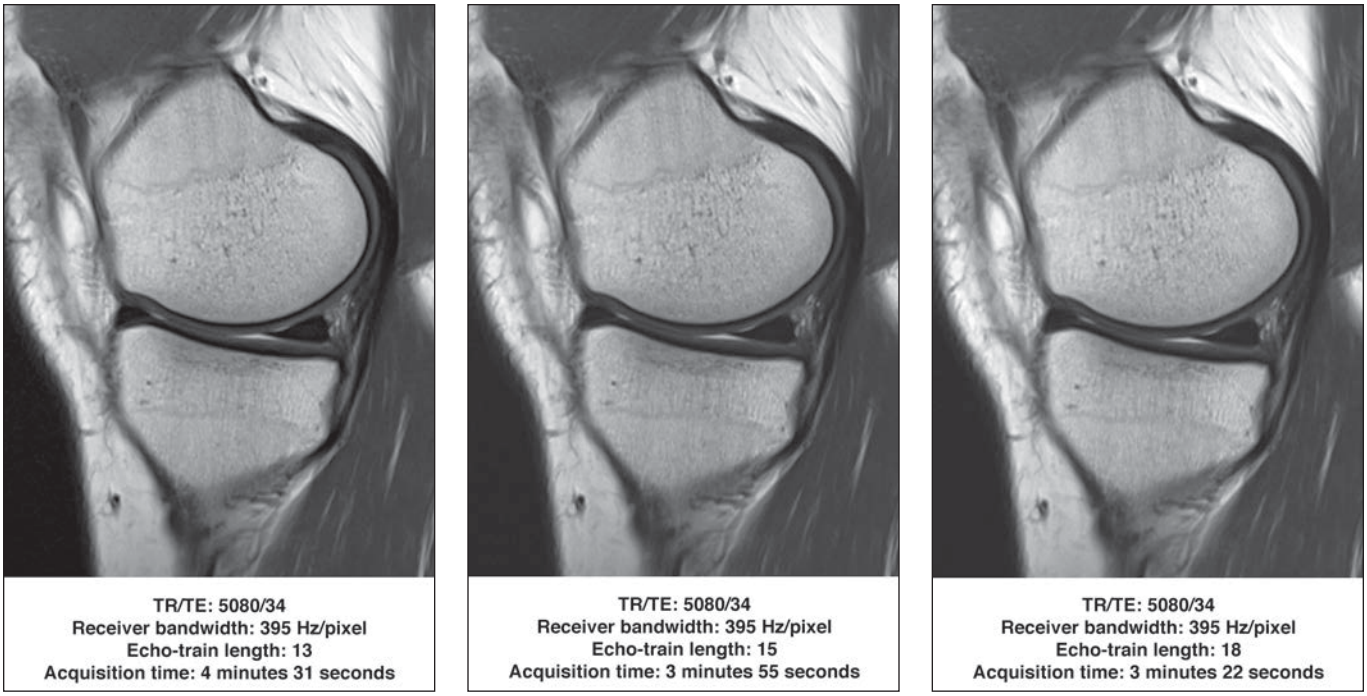


**Fig. 4—**32-year-old healthy man. Effect of echo-train length on acquisition time and image quality using sagittal proton density–weighted turbo spin-echo MR images of knee. When echo-train length was increased from 13 to 18, acquisition time decreased by more than 1 minute, whereas image quality remained constant. Use of longer echo trains and preservation of image quality are afforded through short-echo spacing resulting from use of fast radiofrequency pulses, high gradient performance mode, and higher receiver bandwidth.
**A–C,** MR images obtained at varying echo-train lengths and acquisition times.

**TABLE 2: Effect of Echo-Train Length on Acquisition Time When Using Sagittal Proton Density–Weighted TSE MRI Sequences of the Knee**

| Parameter | Sequence 1 | Sequence 2 | Sequence 3 |
|---|---|---|---|
| Orientation | Sagittal | Sagittal | Sagittal |
| Gradient performance | High | High | High |
| Radiofrequency speed | Fast | Fast | Fast |
| TR (ms) | 5080 | 5080 | 5080 |
| TE (ms) | 34 | 34 | 34 |
| Echo-train length | 13 | 15 | 18 |
| Bandwidth (Hz/pixel) | 395 | 395 | 395 |
| FOV (mm) | 150 × 150 | 150 × 150 | 150 × 150 |
| Matrix size | 386 × 386 | 386 × 386 | 386 × 386 |
| Slice thickness (mm) | 3 | 3 | 3 |
| Voxel size (mm) | 0.4 × 0.4 × 3.0 | 0.4 × 0.4 × 3.0 | 0.4 × 0.4 × 3.0 |
| No. of slices | 30 | 30 | 30 |
| No. of concatenations | 1 | 1 | 1 |
| Phase direction | Head to foot | Head to foot | Head to foot |
| Phase oversampling (%) | 75 | 75 | 75 |
| Flip angle (°) | 150 | 150 | 150 |
| Echo spacing (ms) | 8.6 | 8.6 | 8.6 |
| Acquisition time (min:s) | 4:31 | 3:55 | 3:20 |

Note—TSE = turbo spin-echo.

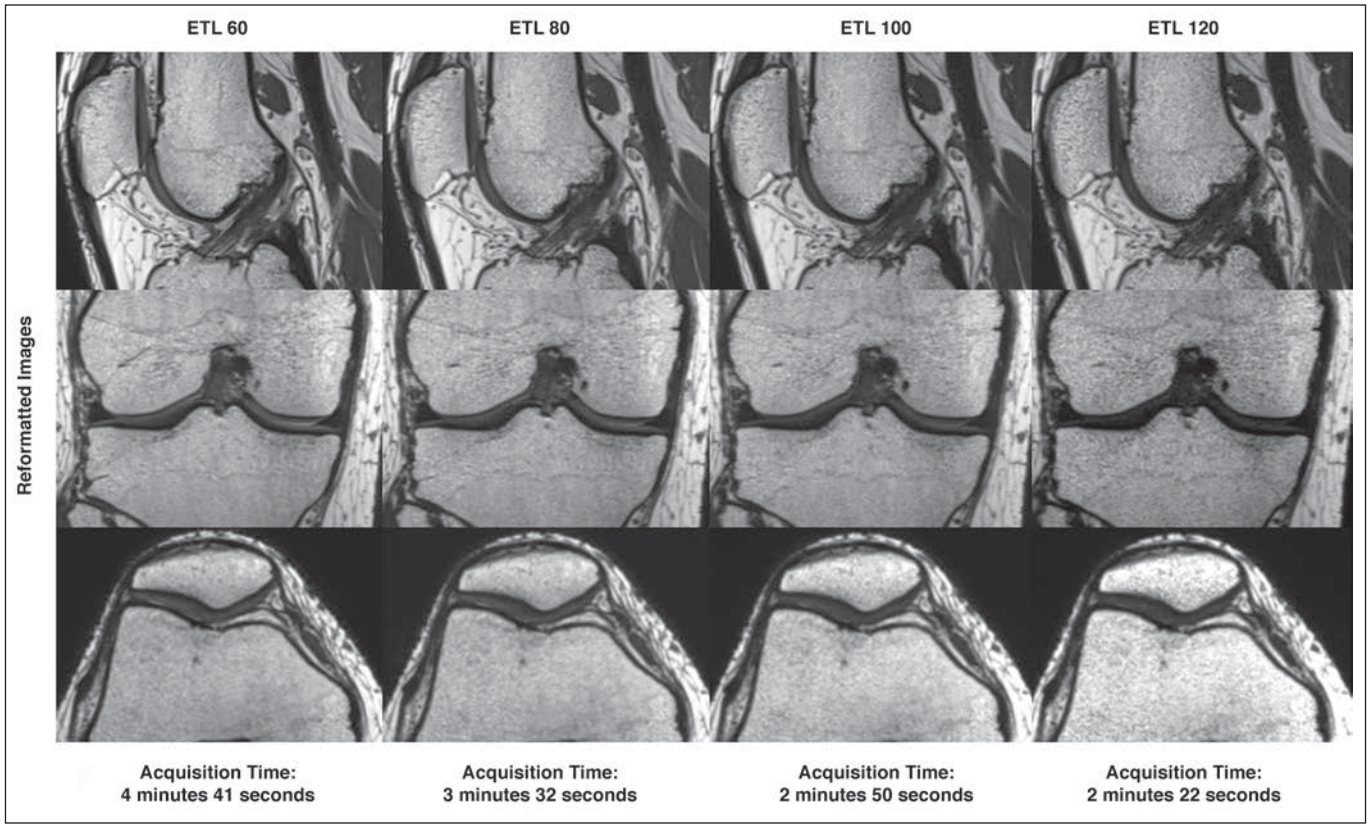


**Fig. 5**—28-year-old healthy man. Effect of echo-train length (ETL) on image quality of 3D turbo spin-echo pulse sequence. All datasets were obtained with 3D sampling perfection with application-optimized contrasts using different flip-angle evolution (SPACE) turbo spin-echo pulse sequence on 3-T MRI system with 15-channel knee coil, with use of following pulse sequence parameters: TR/TE of 900/23, FOV of 16 × 16 cm, matrix of 320 × 320, slice thickness of 0.5 mm, voxel size of 0.5 mm × 0.5 mm × 0.5 mm, 240 slices, anterior-to-posterior phase-encoding direction, flip angle of 120°, 2 × 2–1 controlled aliasing in parallel imaging results in higher acceleration (CAIPIRINHA) acceleration, and receiver bandwidth of 390 Hz/pixel. Series shows trade-off between increasing ETL with decreasing acquisition time and increasing degradation of image quality, which is characterized by decreasing signal-to-noise ratios, decreasing proton density, increasing T2 weightings, introduction of overacceleration artifacts, and degrading quality of multiplanar axial and coronal reformation images.

Another effect of scanning with reduced matrix resolution in the phase direction is the incrementally increasing SNR resulting from reduced phase encoding and increasing voxel size (see equation 1). In practice, matrix resolution phase undersampling of 5%, 10%, 15%, 20%, and 25% results in SNR gains of 3%, 6%, 8%, 12%, and 15%, respectively.

When 2D FSE and TSE pulse sequences are used, small pixel size asymmetries from matrix undersampling in the phase-encoding direction are often barely visible to the human eye (Fig. 6), but they shorten the acquisition time and increase the SNR.

When 3D FSE and TSE pulse sequences are used, asymmetric voxel size may be barely visible in the acquired plane but can have a degrading effect on the quality of multiplanar reformation images.

## Interpolation of Matrix Resolution

Image matrix interpolation describes the process of creating images with a higher matrix resolution than the sampled data initially permit. To reconstruct images with a higher matrix resolution, empty (i.e., zero) filling or estimated data can be added mathematically during or after data acquisition [46]. Interpolation techniques do not add new numeric information; however, interpolation of the matrix resolution can improve edge sharpness and partial volume effects [47]. No direct decrease in acquisition time occurs through interpolation; however, when interpolation is used to compensate for MR images that were acquired with a slightly lower matrix resolution but a shorter acquisition time (see equation 1), indirect savings are achieved (Fig. 7).

In practice, matrix interpolation techniques may not compensate for comparatively larger differences between native and interpolation matrices. Interpolation increases the data size of MR images according to the number of pixels added. Many vendors offer refined k-space– and image-based interpolation algorithms as part of standard software packages. Artificial intelligence–based postprocessing interpolation techniques are an active area of research and may further improve this technique [48].

## Partial Fourier Phase Undersampling

Partial Fourier undersampling techniques permit the reconstruction of complete MR images with only partially sampled MR signals in the phase- or frequency-encoding direction [49]. The techniques exploit the diagonal center-point symmetry of the k-space, which means that in an ideal k-space, one half inversely mirrors the other half (Fig. 8). Theoretically, this means that only one-half of all phase- or frequency-encoded MR signals are

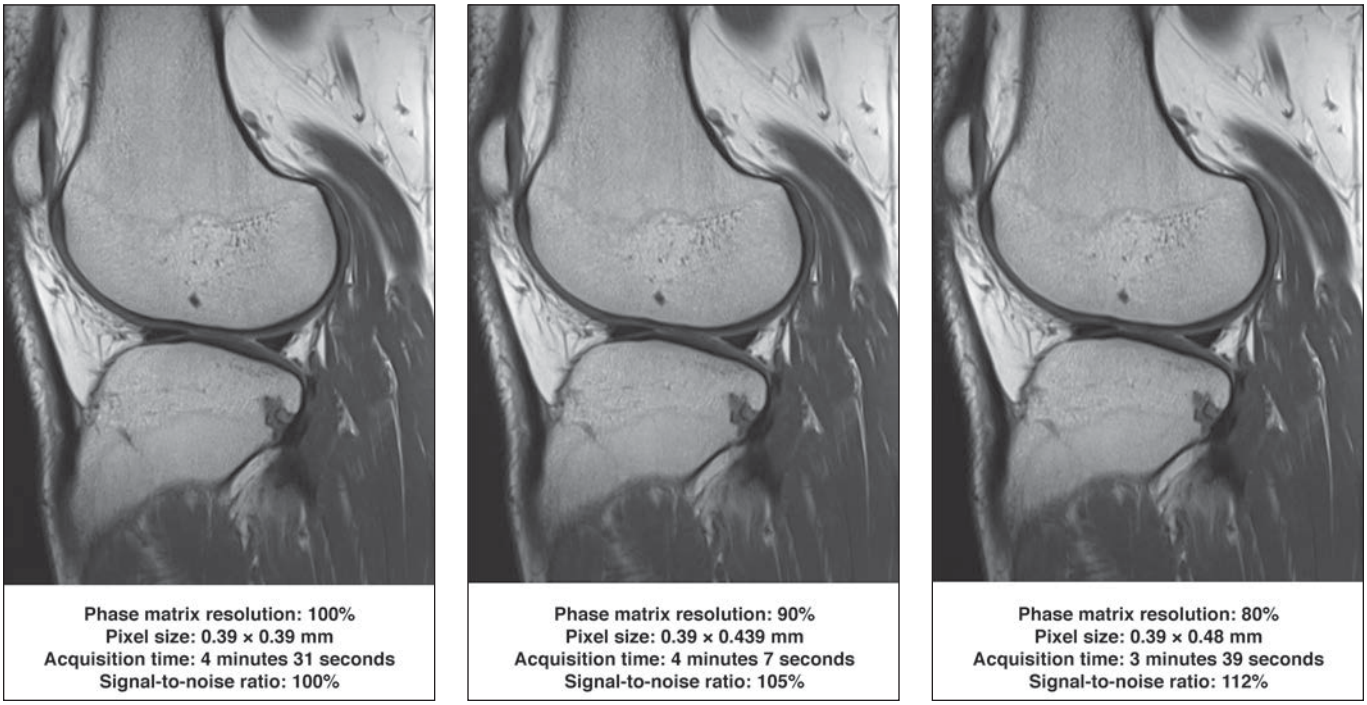


**Fig. 6**—44-year-old healthy man. Effects of matrix resolution phase undersampling. Sagittal intermediate-weighted MR images were obtained using 3-T MRI system and 15-channel knee coil with use of following pulse sequence parameters: TR/TE of 4010/27, FOV of 15 × 15 cm, slice thickness of 2.5 mm, echo-train length of 13, 30 slices, head-to-foot phase-encoding direction, 75% phase oversampling, flip angle of 150°, receiver bandwidth of 395 Hz/pixel.
**A,** MR image obtained with fully sampled 386 × 386 matrix resolution with quadratic pixel size.
**B,** MR image obtained with 90% undersampling, resulting in 386 × 346 matrix with rectangular pixel size, decreased acquisition time, and increased signal-to-noise ratio.
**C,** MR image obtained with 80% phase undersampling, resulting in 386 × 308 matrix with rectangular pixel size, further decrease in acquisition time, and further increase in signal-to-noise ratio. Difference in pixel size may not be perceptible but results in meaningful reduction of acquisition time and net gain of signal-to-noise ratio.

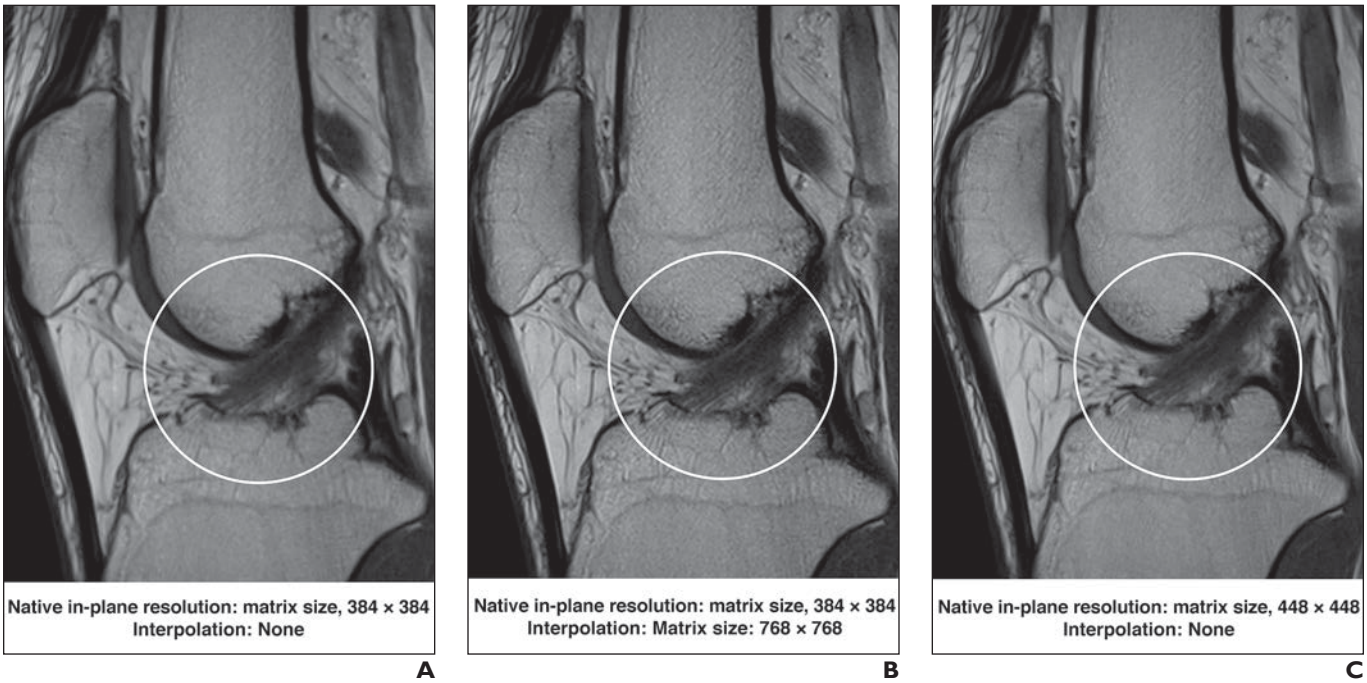


**Fig. 7**—32-year-old healthy man. Effects of matrix interpolation. Sagittal intermediate-weighted MR images were obtained using 3-T MRI system and 15-channel knee coil with use of following pulse sequence parameters: TR/TE of 4010/27, FOV of 15 × 15 cm, slice thickness of 2.5 mm, echo-train length of 13, 30 slices, head-to-foot phase-encoding direction, 75% phase oversampling, flip angle of 150°, and receiver bandwidth of 395 Hz/pixel.
**A**–**C,** Fourfold postprocessing interpolation of native matric size (**A**) results in apparent increase in sharpness (**B**) of edge of intact anterior cruciate ligament fibers (*circles*). Apparent spatial resolution in **B** may be perceived as higher than that of MR image that was sampled with higher spatial resolution and longer acquisition time (**C**).

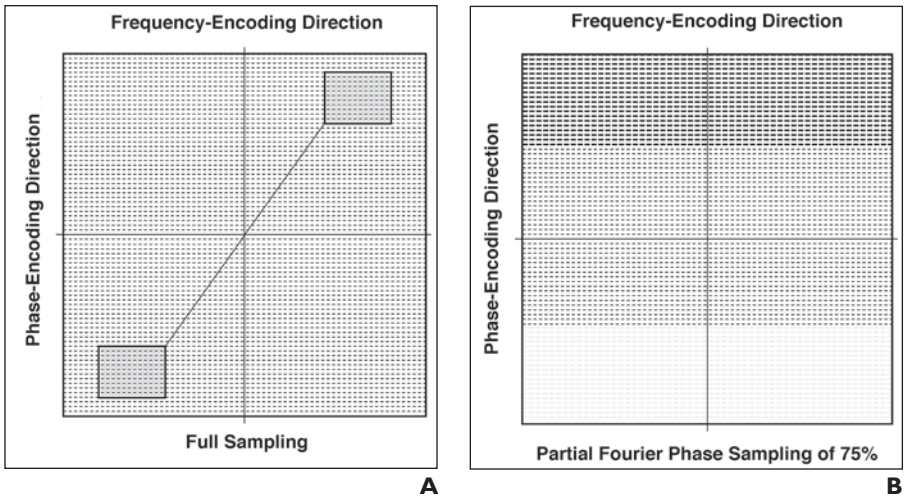


**Fig. 8**—Partial Fourier phase sampling. Horizontal lines represent signal readout with different phase encoding.
**A,** Schematic shows fully sampled k-space. Gray squares indicate diagonal center-point symmetry of k-space with different polarities. Diagonal line denotes center-point symmetry of k-space.
**B,** Schematic shows partial Fourier phase sampling in which only 75% of k-space lines are sampled, and 25% are mathematically transferred from upper half (*darkest gray lines*) to lower half (*light gray lines*) of through center-point symmetry of k-space.

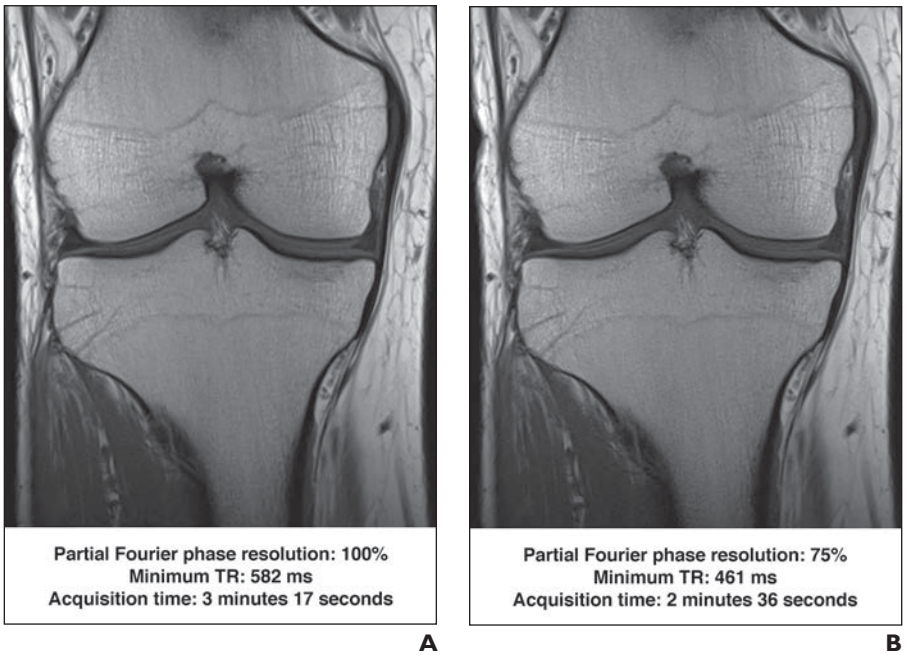


**Fig. 9**—40-year-old healthy woman. Effect of partial Fourier phase acceleration on coronal T1-weighted turbo spin-echo MR images of knee.
**A,** MR image obtained with fully sampled matrix.
**B,** MR image obtained with partial Fourier phase undersampling.

required to create an MR image. However, in practice, at least 55–60% are needed because of small technical imperfections. Some platforms allow predefined increments of partial Fourier phase undersampling (e.g., 75%) (Fig. 8). Other platforms scale the permitted partial Fourier undersampling factor dynamically as a function of TE, which means that for FSE and TSE pulse sequences the amount of permitted Fourier undersampling depends on the TEs of the pulse sequence.

Although the reconstructed images have the full matrix size, the SNR will be lower. Sampling 75% of a 320-phase matrix will result in an approximately 15% reduction in the SNR. Another option is filling unsampled data points with empty data (i.e., zero filling), which will result in a similar decrease in the SNR but will also introduce blur.

Partial Fourier phase techniques shorten the acquisition time because the number of phase-encoded echoes is directly proportional to the acquisition time (see equation 1). Depending on the platform and pulse sequence, other solutions include a reduction in the minimally possible TR (Fig. 9 and Table 3) and TE as well as an increase in the maximum number of echoes within an echo train and in the number of slices.

In comparison with parallel imaging acceleration [50], partial Fourier sampling does not require multichannel array coils and reference lines and therefore is more accessible, is potentially faster at low acceleration factors, and is less motion sensitive. Because the maximum acceleration factor of partial Fourier phase MRI is less than 2, parallel imaging allows higher acceleration factors.

## Combined Use of Widely Accessible Acceleration Techniques

Widely accessible techniques can be applied to accelerated musculoskeletal MRI in various combinations. Table 4 provides a checklist for optimizing FSE and TSE pulse sequences in musculoskeletal MRI protocols with the use of different techniques. All techniques can be applied to create proton density–, T1-, and T2-weighted MR images without and with the use of various fat suppression techniques (Fig. 10 and Table 5). In our prac-

**TABLE 3: Effects of Partial Fourier Phase Undersampling on Acquisition Time When Using Coronal T1-Weighted TSE MRI Sequences of the Knee**

| Parameter | Sequence 1 | Sequence 2 |
|---|---|---|
| Gradient performance | High | High |
| Radiofrequency speed | Fast | Fast |
| Minimum TR (ms) | 582 | 461 |
| TE (ms) | 8 | 8 |
| Echo-train length | 4 | 4[a] |
| Bandwidth (Hz/pixel) | 397 | 397 |
| FOV (mm) | 150 × 150 | 150 × 150 |
| Matrix size | 386 × 386 | 386 × 386 |
| Slice thickness (mm) | 3 | 3 |
| Voxel size (mm) | 0.4 × 0.4 × 3.0 | 0.4 × 0.4 × 3.0 |
| No. of slices | 28 | 28 |
| No. of concatenations[b] | 2 | 2 |
| Partial Fourier phase sampling (%) | — | 75 |
| Phase direction | Head to foot | Head to foot |
| Phase oversampling (%) | 75 | 75 |
| Flip angle (°) | 150 | 150 |
| Echo spacing (ms) | 8.6 | 8.6 |
| Acquisition time (min:s) | 3:17 | 2:36 |

Note—Dash (—) denotes no partial Fourier phase undersampling was applied. TSE = turbo spin-echo.
[a]The new timing afforded by partial Fourier phase sampling would permit an increase in echo-train length from a maximum of 4 to 5 and an acquisition time of 2 minutes 5 seconds. However, an echo-train length of 5 would result in a small increase of T2 weighting and thus may be avoided to preserve sufficient T1 weighting of the resulting MR images.
[b]Two concatenations indicate that the number of slices was acquired in two sets.

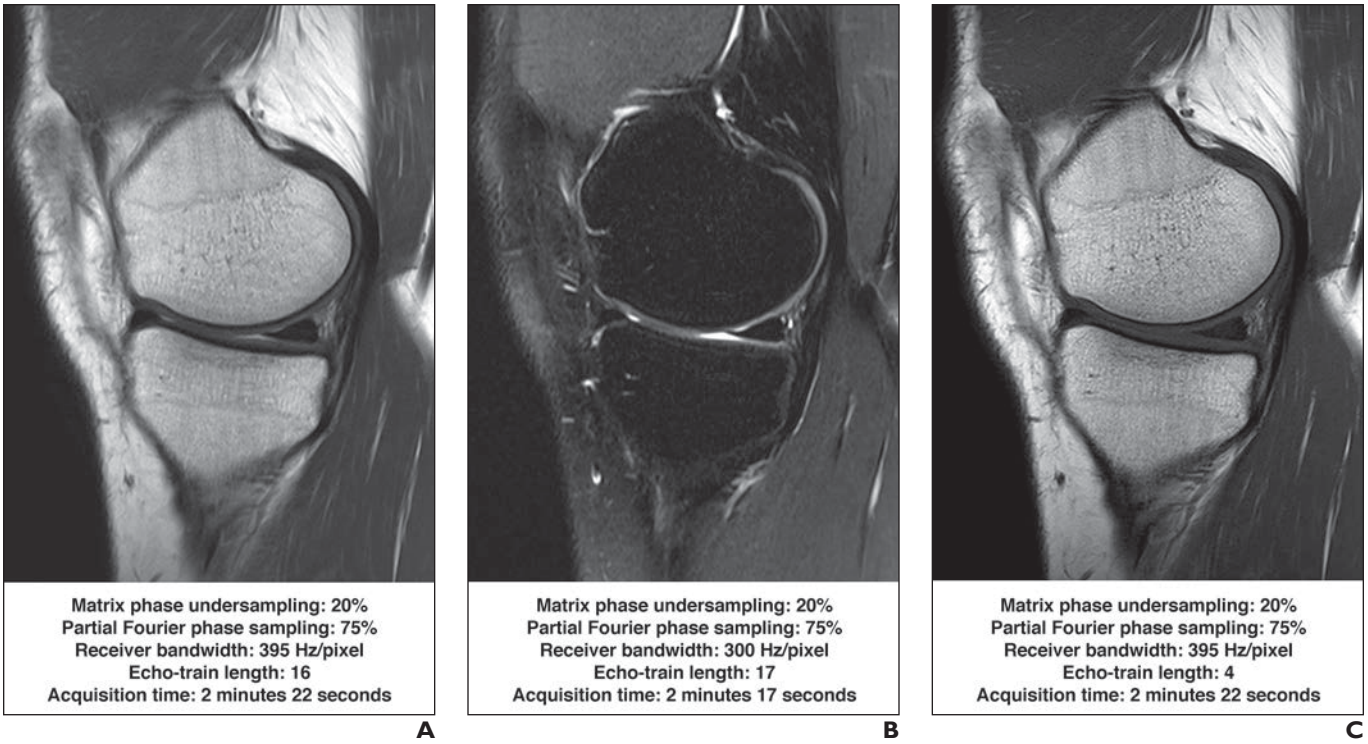


**Fig. 10**—32-year-old healthy man. Combined use of high gradient performance, fast radiofrequency pulses, high-readout bandwidth, long echo trains, matrix resolution phase undersampling, and partial Fourier phase undersampling for acceleration of MRI. Approximately twofold mean acceleration was achieved with retention of sufficient MR signal, contrast resolution and fluid brightness, image sharpness, apparent spatial resolution, and number of slices.
**A,** MR image obtained with intermediate weighting.
**B,** MR image obtained with T2 weighting and spectral fat suppression.
**C,** MR image obtained with T1 weighting.

**TABLE 4: Checklist of Accessible Techniques for Rapid Musculoskeletal MRI**

| Technique | Gain | Effect on Acquisition Time |
|---|---|---|
| Use of FSE or TSE instead of conventional spin-echo pulse sequences | Sampling of multiple echoes per TR with FSE or TSE, rather than sampling of only one echo per TR with conventional spin echo | Acquisition time decreases proportionally to the echo-train length |
| Use of high gradient performance modes | Shortening of echo spacing, which leads to compaction of echo trains | Shorter time to complete echo trains permits shorter acquisition times through lower possible TRs or the use of longer echo trains |
| Use of fast radiofrequency pulses | | |
| Use of high receiver bandwidth | | |
| Use of longer echo trains with proton density– and T2-weighted FSE and TSE pulse sequences | Longer echo trains but same time to complete echo trains requires fewer TR cycles to create the same number of MR images | Acquisition time decreases proportionally to the increased number of echoes with the echo train |
| Undersampling of matrix resolution in phase-encoding direction | Fewer phase-encoding steps are used to create MR images of the same size, while the signal gain increases | Acquisition time decreases proportionally to the percentage of undersampling |
| Interpolation of matrix resolution | Mathematic increase in matrix resolution of MR images | Can indirectly decrease acquisition time if the original images were acquired with a lower matrix resolution |
| Use of partial Fourier phase undersampling | Fewer phase-encoding steps are needed to create MR images with the same size and matrix | Acquisition time decreases proportionally to the percentage of undersampling |

Note—FSE = fast spin-echo, TSE = turbo spin-echo.

**TABLE 5: Accelerated Turbo Spin-Echo Pulse MRI Sequences of the Knee**

| Parameter | Proton Density–Weighted Sequence | T2-Weighted Sequence With Spectral FS | T1-Weighted Sequence |
|---|---|---|---|
| Orientation | Sagittal | Sagittal | Sagittal |
| Gradient performance | High | High | High |
| Radiofrequency speed | Fast | Fast | Fast |
| TR (ms) | 4000 | 4360 | 508 |
| TE (ms) | 34 | 63 | 8 |
| Echo-train length | 16 | 17 | 4 |
| Bandwidth (Hz/pixel) | 395 | 300 | 395 |
| Matrix phase resolution sampling (%) | 80 | 80 | 80 |
| Partial Fourier phase sampling (%) | 75 | 94 | 75 |
| FOV (mm) | 150 × 150 | 150 × 150 | 150 × 150 |
| Matrix size | 386 × 308 | 386 × 308 | 386 × 308 |
| Slice thickness (mm) | 3 | 3 | 3 |
| Voxel size (mm) | 0.4 × 0.5 × 3.0 | 0.4 × 0.5 × 3.0 | 0.4 × 0.5 × 3.0 |
| No. of slices | 30 | 30 | 30 |
| No. of concatenations | 1 | 1 | 2 |
| Phase direction | Head to foot | Head to foot | Head to foot |
| Phase oversampling (%) | 75 | 90 | 75 |
| Flip angle (°) | 150 | 150 | 150 |
| Echo spacing (ms) | 8.6 | 7.8 | 8.6 |
| Acquisition time (min:s) | 2:22 | 2:17 | 2:05 |
| Unaccelerated acquisition time (min:s)[a] | 4:16 | 4:00 | 4:43 |

Note—Accelerated sequences were afforded by the combined use of high gradient performance, fast radiofrequency pulses, high-readout bandwidth, long echo trains, matrix resolution phase undersampling, and partial Fourier phase undersampling using a clinical 3-T MRI system with a slew rate of 200 T/m/s, a gradient strength of 45 mT/m, and a knee coil with one transmit and 15 receiver channels. FS = fat suppression.

[a]Acquisition involved use of regular gradient performance and radiofrequency pulses, high-readout bandwidth, echo-train length of 13 for protein density– and T2-weighted fat-suppressed MR images, echo-train length of 4 for T1-weighted MR images, and full k-space sampling.

tice, the most effective techniques for accelerating musculoskeletal MRI examinations are the combined use of matrix resolution phase undersampling of 20–25%, fast radiofrequency pulses, a high gradient performance mode, and high receiver bandwidth that shortens echo spacing with concomitant use of ETLs of 10–16 and retention of TRs of 3500–5000 ms for proton density–weighted and T2-weighted FSE and TSE pulse sequences.

## Conclusion

The combination of modern scanner technology and a multitude of widely accessible techniques can substantially accelerate musculoskeletal MRI examinations while retaining image quality, comprehensiveness, and diagnostic performance. Optimized efficiency is a cornerstone for adding value to musculoskeletal MRI by increasing availability and accessibility, improving tolerability for adult and pediatric patients, reducing motion artifacts, decreasing the need for sedation and anesthesia, and augmenting throughput.

## References


1. Agten CA, Sutter R, Buck FM, Pfirrmann CW. Hip imaging in athletes: sports imaging series. *Radiology* 2016; 280:351–369
2. Guermazi A, Roemer FW, Robinson P, Tol JL, Regatte RR, Crema MD. Imaging of muscle injuries in sports medicine: sports imaging series. *Radiology* 2017; 282:646–663
3. Linklater JM, Hayter CL, Vu D. Imaging of acute capsuloligamentous sports injuries in the ankle and foot: sports imaging series. *Radiology* 2017; 283:644–662
4. Bucknor MD, Stevens KJ, Steinbach LS. Elbow imaging in sport: sports imaging series. *Radiology* 2016; 279:12–28
5. Naraghi AM, White LM. Imaging of athletic injuries of knee ligaments and menisci: sports imaging series. *Radiology* 2016; 281:23–40
6. Ahlawat S, Fritz J, Morris CD, Fayad LM. Magnetic resonance imaging biomarkers in musculoskeletal soft tissue tumors: review of conventional features and focus on nonmorphologic imaging. *J Magn Reson Imaging* 2019; 50:11–27
7. Lecouvet FE, Whole-body MR imaging: musculoskeletal applications. *Radiology* 2016; 279:345–365
8. Coris EE, Zwygart K, Fletcher M, Pescasio M. Imaging in sports medicine: an overview. *Sports Med Arthrosc Rev* 2009; 17:2–12
9. Piccolo CL, Galluzzo M, Ianniello S, et al. Pediatric musculoskeletal injuries: role of ultrasound and magnetic resonance imaging. *Musculoskelet Surg* 2017; 101(suppl 1):85–102
10. Hynes JP, Walsh J, Farrell TP, Murray AS, Eustace SJ. Role of musculoskeletal radiology in modern sports medicine. *Semin Musculoskelet Radiol* 2018; 22:582–591
11. Black BR, Chong LR, Potter HG. Cartilage imaging in sports medicine. *Sports Med Arthrosc Rev* 2009; 17:68–80
12. van Beek EJR, Kuhl C, Anzai Y, et al. Value of MRI in medicine: more than just another test? *J Magn Reson Imaging* 2019; 49:e14–e25
13. Runge VM, Richter JK, Heverhagen JT. Speed in clinical magnetic resonance. *Invest Radiol* 2017; 52:1–17
14. Garwood ER, Recht MP, White LM. Advanced imaging techniques in the knee: benefits and limitations of new rapid acquisition strategies for routine knee MRI. *AJR* 2017; 209:552–560
15. Gyftopoulos S, Lin D, Knoll F, Doshi AM, Rodrigues TC, Recht MP. Artificial intelligence in musculoskeletal imaging: current status and future directions. *AJR* 2019; 213:506–513
16. Fritz F, Guggenberger R, Del Grande F. Rapid musculoskeletal MRI in 2021: clinical application of advanced accelerated techniques. *AJR* 2021 (in press)
17. Geethanath S, Vaughan JT Jr. Accessible magnetic resonance imaging: a review. *J Magn Reson Imaging* 2019; 49:e65–e77
18. Anzai Y, Minoshima S, Lee VS. Enhancing value of MRI: a call for action. *J Magn Reson Imaging* 2019; 49:e40–e48
19. Parker L, Nazarian LN, Carrino JA, et al. Musculoskeletal imaging: medicare use, costs, and potential for cost substitution. *J Am Coll Radiol* 2008; 5:182–188
20. Tulipan J, Beredjiklian P, Gandhi JS, Liss F, Rivlin M. Changes in Medicare reimbursement for advanced upper extremity imaging. *J Hand Surg Am* 2019; 44:246 e1–e7
21. Beker K, Garces-Descovich A, Mangosing J, Cabral-Goncalves I, Hallett D, Mortele KJ. Optimizing MRI logistics: prospective analysis of performance, efficiency, and patient throughput. *AJR* 2017; 209:836–844
22. Recht MP, Block KT, Chandarana H, et al. Optimization of MRI turnaround times through the use of dockable tables and innovative architectural design strategies. *AJR* 2019; 212:855–858
23. Zobel MS, Borrello JA, Siegel MJ, Stewart NR. Pediatric knee MR imaging: pattern of injuries in the immature skeleton. *Radiology* 1994; 190:397–401
24. Mossa-Basha M, Meltzer CC, Kim DC, Tuite MJ, Kolli KP, Tan BS. Radiology department preparedness for COVID-19: *Radiology* Scientific Expert Panel. *Radiology* 2020; 296:E106–E112
25. Vasanawala SS, Alley MT, Hargreaves BA, Barth RA, Pauly JM, Lustig M. Improved pediatric MR imaging with compressed sensing. *Radiology* 2010; 256:607–616
26. Tuite MJ, Kransdorf MJ, Beaman FD, et al. ACR Appropriateness Criteria acute trauma to the knee. *J Am Coll Radiol* 2015; 12:1164–1172
27. Link TM, Patel R. The need for short MRI examinations: a musculoskeletal perspective. *J Magn Reson Imaging* 2019; 49:e49–e50
28. Chew FS, Mulcahy MJ, Porrino JA, Mulcahy H, Relyea-Chew A. Prevalence of burnout among musculoskeletal radiologists. *Skeletal Radiol* 2017; 46:497–506
29. Gold GE, Han E, Stainsby J, Wright G, Brittain J, Beaulieu C. Musculoskeletal MRI at 3.0 T: relaxation times and image contrast. *AJR* 2004; 183:343–351
30. Maubon AJ, Ferru JM, Berger V, et al. Effect of field strength on MR images: comparison of the same subject at 0.5, 1.0, and 1.5 T. *RadioGraphics* 1999; 19:1057–1067
31. Shapiro L, Harish M, Hargreaves B, Staroswiecki E, Gold G. Advances in musculoskeletal MRI: technical considerations. *J Magn Reson Imaging* 2012; 36:775–787
32. Potter HG, Schachar J. High resolution noncontrast MRI of the hip. *J Magn Reson Imaging* 2010; 31:268–278
33. Lee SC, Endo Y, Potter HG. Imaging of groin pain: magnetic resonance and ultrasound imaging features. *Sports Health* 2017; 9:428–435
34. Weishaupt D, Köchli VD, Marincek B. How does MRI work? An introduction to the physics and function of magnetic resonance imaging, 2nd ed. Springer-Verlag, 2006
35. Mugler JP 3rd. Optimized three-dimensional fast-spin-echo MRI. *J Magn Reson Imaging* 2014; 39:745–767
36. Del Grande F, Delcogliano M, Guglielmi R, et al. Fully automated 10-minute 3D CAIPIRINHA SPACE TSE MRI of the knee in adults: a multicenter, multireader, multifield-strength validation study. *Invest Radiol* 2018; 53:689–697
37. Fritz J, Raithel E, Thawait GK, Gilson W, Papp DF. Six-fold acceleration of high-spatial resolution 3D SPACE MRI of the knee through incoherent k-space undersampling and iterative reconstruction: first experience. *Invest Radiol* 2016; 51:400–409
38. Hennig J, Nauerth A, Friedburg H. RARE imaging: a fast imaging method

for clinical MR. *Magn Reson Med* 1986; 3:823–833
39. Del Grande F, Santini F, Herzka DA, et al. Fat-suppression techniques for 3-T MR imaging of the musculoskeletal system. *RadioGraphics* 2014; 34:217–233
40. Fritz J, Lurie B, Potter HG. MR imaging of knee arthroplasty implants. *RadioGraphics* 2015; 35:1483–1501
41. Fritz J, Lurie B, Miller TT, Potter HG. MR imaging of hip arthroplasty implants. *RadioGraphics* 2014; 34:E106–E132
42. Allison J, Yanasak N. What MRI sequences produce the highest specific absorption rate (SAR), and is there something we should be doing to reduce the SAR during standard examinations? *AJR* 2015; 205:[web]W140
43. Alsop DC. The sensitivity of low flip angle RARE imaging. *Magn Reson Med* 1997; 37:176–184
44. Turner R. Gradient coil design: a review of methods. *Magn Reson Imaging* 1993; 11:903–920
45. Zhang B, Yen YF, Chronik BA, McKinnon GC, Schaefer DJ, Rutt BK. Peripheral nerve stimulation properties of head and body gradient coils of various sizes. *Magn Reson Med* 2003; 50:50–58
46. Badar F, Xia Y. Image interpolation improves the zonal analysis of cartilage T2 relaxation in MRI. *Quant Imaging Med Surg* 2017; 7:227–237
47. Bernstein MA, Fain SB, Riederer SJ. Effect of windowing and zero-filled reconstruction of MRI data on spatial resolution and acquisition strategy. *J Magn Reson Imaging* 2001; 14:270–280
48. Chaudhari AS, Stevens KJ, Wood JP, et al. Utility of deep learning super-resolution in the context of osteoarthritis MRI biomarkers. *J Magn Reson Imaging* 2020; 51:768–779
49. McGibney G, Smith MR, Nichols ST, Crawley A. Quantitative evaluation of several partial Fourier reconstruction algorithms used in MRI. *Magn Reson Med* 1993; 30:51–59
50. Deshmane A, Gulani V, Griswold MA, Seiberlich N. Parallel MR imaging. *J Magn Reson Imaging* 2012; 36:55–72